

CONF 900803--3

BNL-NUREG--43991

Received by OSTI

DE90 008579

HEAT TRANSFER BETWEEN STRATIFIED LIQUIDS WITH BUBBLING
ACROSS THE INTERFACE

MAR 26 1990

G.A. Greene
Brookhaven National Laboratory
Upton, New York 11973J.C. Chen
Lehigh University
Bethlehem, Pennsylvania 18015T.F. Irvine, Jr.
State University of New York
Stony Brook, New York 11794

ABSTRACT

A situation that arises in the chemical, metallurgical, and nuclear power industries is one in which two overlying immiscible liquids are stirred by gas bubbles rising across their interface. Due to the gas bubbling, there are three mixture configurations that may occur which depend primarily upon the physical and transport properties of the two liquids, and the droplet and bubble dynamics. These are the stratified, partially-mixed, and fully-mixed configurations. A model is presented for heat transfer between the liquids in the stratified state. A criterion for the onset of entrainment and a model for the rate of mass entrainment per bubble are also presented. These models are combined to develop a predictive capability for the heat transfer across the liquid-liquid interface in the partially-mixed and stratified regimes.

1. DESCRIPTION OF PHENOMENA

Consider the case of two immiscible liquids in initially stratified layers and agitated by rising gas bubbles as illustrated in Figures 1 a-c. As gas bubbles rise upwards through the liquid-liquid interface, they not only disturb the temperature gradients on both sides of the interface, but may entrain the lower, heavy liquid into the upper, lighter layer, further increasing the heat transfer from liquid to liquid. If the rising bubbles are not able to support entrainment, the stratified state will prevail, and heat transfer will be across a well-defined interface between two well-mixed pools at different temperatures. This is the configuration presented in Figure 1a.

Under some circumstances, the rising gas bubbles not only agitate the liquid-liquid interface but also drive a mass transfer process by entraining the lower heavy liquid upwards in the wakes of the rising gas bubbles. If the rate of entrainment of the lower phase can be balanced by the rate of droplet settling (or de-entrainment), a partially mixed configuration will result in which the liquid-liquid interface will be preserved between a homogenous lower layer and a heterogeneous upper mixture layer. This is the pool configuration presented in Figure 1b.

*Work performed under the auspices of the U.S.
Nuclear Regulatory Commission

If the rate of entrainment is greater than the rate of settling of the entrained droplets, the two liquids will form a pool that is fully mixed, or fully entrained; there will only be one heterogeneous liquid layer and the concept of interlayer heat transfer will not be applicable. This is the configuration that is presented in Figure 1c. This configuration will not be discussed in this paper.

2. HEAT TRANSFER IN STRATIFIED CONFIGURATION

If conditions are such that entrainment of the lower fluid into the upper fluid cannot be supported by the rising gas bubbles, the liquid layers will remain stratified as illustrated in Figure 1a. In this stratified configuration, the rate of heat transfer between the two layers is controlled by the rate of bubble agitation at the liquid-liquid interface. It was hypothesized by Szekely [1963] that the interfacial heat transfer is a surface renewal phenomenon. As the rising gas bubbles cross the interface, they eliminate the temperature gradients

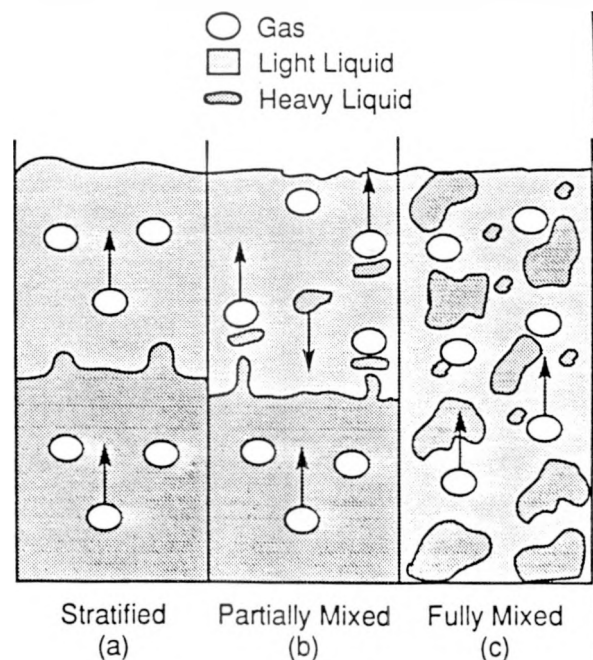


Fig. 1 Configurations of Multifluid Bubbling Pools

MASTER

DISTRIBUTION OF THIS DOCUMENT IS UNLIMITED

DISCLAIMER

This report was prepared as an account of work sponsored by an agency of the United States Government. Neither the United States Government nor any agency thereof, nor any of their employees, makes any warranty, express or implied, or assumes any legal liability or responsibility for the accuracy, completeness, or usefulness of any information, apparatus, product, or process disclosed, or represents that its use would not infringe privately owned rights. Reference herein to any specific commercial product, process, or service by trade name, trademark, manufacturer, or otherwise does not necessarily constitute or imply its endorsement, recommendation, or favoring by the United States Government or any agency thereof. The views and opinions of authors expressed herein do not necessarily state or reflect those of the United States Government or any agency thereof.

DISCLAIMER

Portions of this document may be illegible in electronic image products. Images are produced from the best available original document.

on both sides of the interface, creating a sudden step in temperature across the interface, analogous to the instantaneous contact temperature when two semi-infinite solids are suddenly brought together. After the departure of the bubble, heat conduction in each fluid causes the temperature gradients to be reestablished. The transient growth of the interfacial temperature gradients would continue until interrupted by the arrival of the next bubble, at which point the process would be repeated locally on a periodic basis. Szekely developed an analytical solution for the surface renewal heat transfer coefficient for each side of the interface (representing the heat flux divided by the average bulk layer-to-interface temperature difference) by integrating the time-dependent heat flux on each side of the interface over the period of arrival of successive bubbles. He arrived at the following result for the heat transfer coefficient on each side of the interface,

$$h_i = 1.69 \left[\frac{\rho_c c_p k_j j_g}{r_b} \right]^{1/2} \quad (1)$$

which can be cast in dimensionless form as,

$$Nu_i = 1.69 Re_i^{1/2} Pr_i^{1/2} \quad (2)$$

where $Re_i = j_g r_b / \nu$ and $i = 1$ or 2 , representing the upper or lower liquid layer, respectively. The overall heat transfer would be evaluated by summing the two series resistances on both sides of the interface. Due to the absence of data with which to evaluate this model, Greene and Irvine [1988a] performed an experimental investigation into heat transfer between overlying, stratified immiscible liquids with bubble agitation. The fluids that were tested were water, and 10cs. and 100cs. silicone oils over a layer of mercury. Mercury was used as the lower fluid to prevent entrainment and to present a minimal resistance to heat transfer; therefore, the measured overall heat transfer coefficient would be approximately equal to the surface renewal heat transfer coefficient on the water or oil side of the interface. Three sets of experiments were performed. The experimental data were non-dimensionalized as in Equation 2 and an empirical correlation was developed. The resulting correlation is given by,

$$Nu_i = 1.95 Re_i^{0.72} Pr_i^{0.72} \quad (3)$$

This is the model that is recommended for surface renewal heat transfer driven by gas bubbling in the absence of mass entrainment.

3. ONSET OF BUBBLE-INDUCED ENTRAINMENT

Experiments with liquids such as water or light oils over a pool of mercury (and other heavy metals as well) have shown that the stratified configuration is possible, even under the influence of gas bubbling across the interface. However, there is evidence from other studies [Mercier, 1974; Mori, 1977; Epstein, 1981; Suter, 1988] that indicate that with some fluid pairs, the gas bubbling can drive mass transfer across the interface if some threshold entrainment condition is satisfied. Mercier et al. [1974] report on visual observations in which a minimum bubble volume threshold was observed for

onset of entrainment between water and a variety of mineral oils. A similar observation is reported by Mori et al. [1977] who observed a minimum bubble volume for penetration of a glycerol-R113 interface. Epstein et al. [1981] report that the onset of mixing and stratification is only a function of the fluid densities, while Suter et al. [1988] developed a jet stability criterion based upon both liquid density and interfacial tension.

There still remains a shortage of data with which to evaluate these modeling approaches for entrainment onset or to develop a generalized modeling approach which would be applicable to all fluid pairs. As a result, Greene et al. [1988b] performed a systematic experimental and analytical investigation of the conditions for the onset of mass entrainment across a stratified liquid-liquid interface due to single rising gas bubbles. Experiments were performed for eight fluid pairs with single air bubbles. The bubble volumes in the entrainment onset experiments covered over three orders of magnitude. A sample of the experimental data for onset of entrainment is illustrated in Figure 2 for four of the eight fluid pairs tested. For each of the fluid pairs, a distinct bubble volume at which entrainment onset occurred was observed. The onset volume was observed, however, to be strongly dependent upon the fluid pair, ranging from 0.002 cm³ for acetone/glycerine to 1.0 cm³ for water/bromoform. (Note: an anomalous condition was observed for acetone/glycerine in which two onset volumes were encountered; this has not been resolved.)

An analytical criterion for the prediction of entrainment onset was developed, based upon a static force balance on the bubble/liquid system as it attempts to levitate a column of the lower, heavy liquid, and interfacial tension which acts to restrain the entrainment. Stated in words, when the net upward buoyancy force on the lower fluid exceeds the restoring force due to gravity and interfacial tension, entrainment by single rising gas bubbles is possible. The mathematical criterion for onset of entrainment that was developed is given by the dimensionless inequality,

$$\omega > \frac{V_{\infty}}{V_g^*} \equiv \left[\frac{2(\rho_1 - \rho_g)}{(3\rho_1 - \rho_2 - 2\rho_g)} \right]^{3/2} \quad (4)$$

where ω is the dimensionless bubble volume equal to V_b/V_g^* , V_b is the bubble volume, V_g^* is the necessary bubble volume to penetrate the interface, and V_{∞} is the entrainment onset bubble volume. These are defined as

$$V_{\infty} = \left[\frac{7.8 \sigma_{12}}{(3\rho_1 - \rho_2 - 2\rho_g)g} \right]^{3/2} \quad (5)$$

and

$$V_g^* = \left[\frac{3.9 \sigma_{12}}{(\rho_1 - \rho_g)g} \right]^{3/2} \quad (6)$$

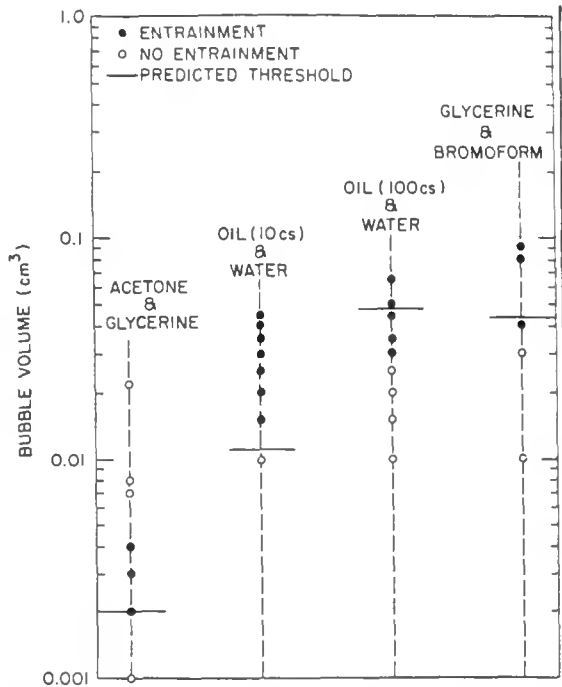


Fig. 2 Comparison of Entrainment Onset Model and Data

The proposed theoretical criterion (Eqns. 4-6), with no empirical parameters, was found to predict the experimental measurements with good agreement over the entire test range, as shown in Figure 2.

4. RATE OF BUBBLE-INDUCED ENTRAINMENT

There is clear evidence in the literature that entrainment between overlying immiscible liquid layers by gas bubbling from below occurs for some fluid pairs, and is a function of the bubble volume as well as the physical and transport properties of the liquids and the gas. This is the configuration shown schematically in Figure 1b. That the rate of entrainment increases with increasing bubble volume for a particular pair of fluids is reported by Poggi et al. [1969], Cheung et al. [1986], Veeraburus and Philbrook [1959], and Mori et al. [1977]. Mori et al. [1977] present data for glycerol-R113 which demonstrate an increase in entrained volume with an increase in bubble volume and a decrease in the viscosity of the light (upper) liquid. Aspects of entrainment mechanisms by films and bubble transport were observed by Poggi et al. [1969], Veeraburus et al. [1959], and Mori et al. [1977]. Cheung et al. [1986] made observations that the entrainment could be affected by non-uniform gas bubbling. A physically-based and general model for the volume entrained by gas bubbles rising across a stratified, liquid-liquid interface which would be applicable to a wide range of fluid pairs was not presented in any of the references cited. As a result, Greene et al. [1990] performed a systematic experimental investigation of the parameters that contribute to the volume of heavy liquid that can be entrained by a gas bubble rising across a liquid-liquid interface to develop a general entrainment rate model. Experiments were performed

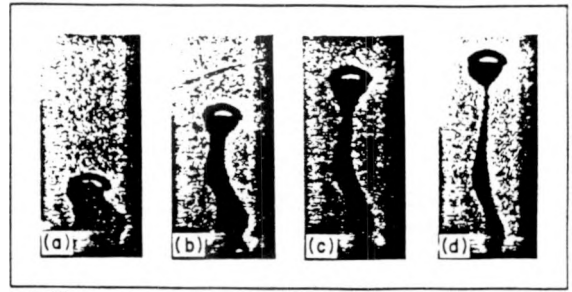


Fig. 3 Stages of Entrainment Phenomenon:
a) Penetration, b) Elongation, c) Necking Down,
d) Entrainment

with eight separate fluid pairs and single air bubbles as previously described for the entrainment onset studies [Greene et al. 1988b]. Single air bubbles of a precise volume were charged into the apparatus and allowed to rise through the liquid interface. The gas bubble volume covered the range from entrainment onset to 4.0 cm³. Both photographic and quantitative measurements were made on the same fluid pairs that were considered in the entrainment onset experiments. For bubbles greater than the entrainment onset threshold, the volume of the lower, heavy fluid was captured and measured. High speed photographic studies, as illustrated in Figures 3 a-d, were found useful in identifying the stages of the entrainment process: these are identified as the bubble penetration, elongation, necking down, and entrainment stages. A sample of the experimental data for the volume of heavy, lower liquid entrained by rising gas bubbles is illustrated in Figure 4 for two of the eight fluid pairs tested. The results in Figure 4 illustrate the effect of considering variation in the light liquid density only. Similar observations were made for the effect of the heavy liquid density, light and heavy liquid viscosities, and interfacial tension. The experimental results clearly indicate that the volume of entrainment from the lower pool into the upper pool by a discreet gas bubble is a complicated function of the gas bubble volume, densities and viscosities of both liquids, and the interfacial tension between the two liquids. An analysis based upon a static force balance was developed to predict the maximum volume that can be entrained, neglecting inertial forces as,

$$V_{m.o.} = \frac{V_g(\rho_1 - \rho_2) - (\sigma_{12}/g)(12\pi^2 V_g)^{1/3}}{(\rho_2 - \rho_1)} \quad (7)$$

One can consider an entrainment efficiency, ϵ , by taking the ratio of the actual measured entrained volume, V_e , to the maximum entrainable volume, $V_{m.o.}$

$$\epsilon = V_e/V_{m.o.} \quad (8)$$

It is reasonable to expect that any inefficiencies in the entrainment process would be associated with the size and character of the bubble wakes. The bubble wakes are affected by Re_1 and Re_2 , the bubble Reynolds numbers in the upper (1) and lower (2)

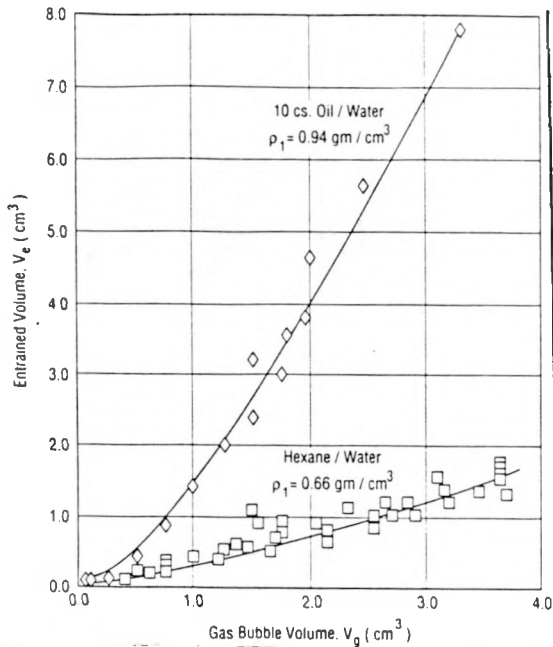


Fig. 4 Effect of Light Liquid Density on Entrainment

liquids, respectively. A functional relationship for the entrainment efficiency was sought of the form, $\epsilon = f(\phi, Re_1, Re_2)$, where ϕ is the dimensionless excess bubble volume beyond that required for onset of entrainment,

$$\phi = \frac{V_g - V_{g0}}{V_{g0}} \quad (9)$$

The final relationship was found to be,

$$\frac{\phi}{\epsilon} Re_1^{0.119} Re_2^{0.380} = 806 \phi^{0.848} \quad (10)$$

This correlation and the experimental data, as illustrated in Figure 5, are found to be in good agreement.

5. OVERALL INTERLAYER HEAT TRANSFER WITH ENTRAINMENT

In order to evaluate the magnitude of the heat transfer between overlying immiscible liquid layers with bubbling induced entrainment across the interface, the configuration shown in Figure 1b, it is necessary to calculate the component due to surface renewal as well as that due to the entrained mass. The total heat transferred between the two liquid layers is assumed to be the sum of the heat transfer across the interface and the heat transfer from the entrained drops of the lower, heavy fluid while suspended in the upper layer. The overall surface renewal heat transfer coefficient, h_{sr} , is constructed by summing the series resistances to heat transfer on both sides of the interface, h_1 and h_2 , as follows:

$$h_{sr}^{-1} = \left[\frac{1}{h_1} + \frac{1}{h_2} \right] \quad (11)$$

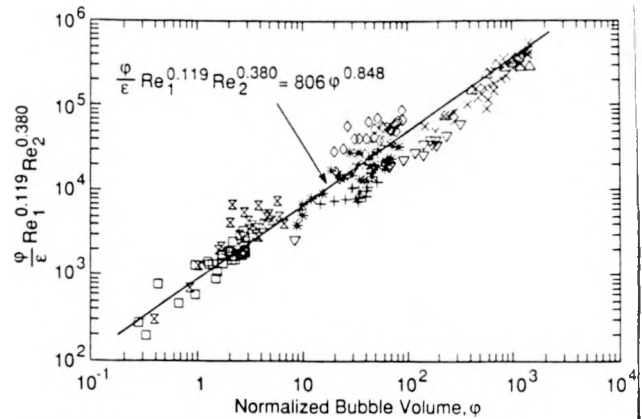


Fig. 5 Correlation of Entrainment Data: \square -Water/Bromoform, \times -100 cs. Silicone Oil/Bromoform, ∇ -10 cs. Silicone Oil/Water, $*$ -Water/R11, $+$ -100 cs. Silicone Oil/Water, \diamond -Glycerine/Bromoform, Δ -Acetone/Glycerine, \times -Hexane/Water

Both h_1 and h_2 can be computed from the surface renewal heat transfer correlation, Equation 3, by simply substituting the fluid properties appropriate to the continuous fluid on each side of the interface.

The heat transferred by the entrained droplets while suspended in the upper, light liquid layer is modeled as a fraction of total excess (or deficit) enthalpy transferred from the drops to the continuous liquid. This can be represented in terms of an entrainment heat transfer coefficient, h_e , as follows:

$$h_e = K \rho_2 C_{p2} j_e \quad (12)$$

where j_e is the superficial (volumetric) entrainment flux, analogous to the superficial gas velocity, j_g ($=$ volumetric gas flux/interfacial cross-sectional area). The superficial entrainment flux, j_e , is defined as the product of the superficial gas velocity and the ratio of entrained volume per bubble to the bubble volume:

$$j_e = j_g \left(\frac{V_e}{V_g} \right) \quad (13)$$

Both Equations 11 and 13 illustrate the importance of not only the physical and transport properties of both liquids, but the size of the rising bubbles as well, in evaluating the heat transfer under entraining conditions. The size of the bubbles was directly measured in the course of these tests. The parameter K in Equation 12 is an efficiency factor for the droplet-liquid heat transfer which represents the actual fraction of excess enthalpy transferred from the drop to the surrounding liquid. For the experimental data to be presented, K was found to be almost always nearly equal to one, and will be assumed equal to one for this model. The total interlayer heat transfer coefficient can now be represented by summing Equations 11 and 12 as follows,

$$h_T = h_{sr} + \rho_2 C_{p2} j_e \quad (14)$$

where the first term on the right hand side is the contribution due to surface renewal effects and the second term is due to mass transport effects. This heat transfer coefficient is multiplied by the overall temperature difference from bulk layer to bulk layer to calculate the overall heat flux.

It is possible to non-dimensionalize Equation 14 by multiplying both sides by the quantity (d_b/k_2) , resulting in the following dimensionless form of the total interlayer heat transfer model,

$$Nu_T = Nu_{SR} + Re_o Pr_2 \quad (15)$$

where $Nu_T = h_T d_b / k_2$, $Nu_{SR} = h_{SR} d_b / k_2$, $Re_o = j_o d_b / \nu_2$, and Pr_2 is the Prandtl number of the lower, heavy liquid layer. This form of the model may be useful for evaluating data for additional fluid pairs as they become available.

In order to evaluate the model for total interlayer heat transfer with entrainment (Figure 1b, Equation 14), a series of two heat transfer experiments were performed [Greene and Schwarz, 1982]. The experiments utilized 10 cs. silicone oil over water with gas bubbling from a porous frit installed in the test section base. The heat transfer coefficient that was measured was the net overall heat transfer coefficient, including both the surface renewal and entrainment components. The resulting experimental heat transfer data are listed in Table 1 and shown graphically in Figure 6. The heat transfer coefficient was then calculated by Equation 14 and compared to the measured data, as shown in Figure 6. The model was shown to be in good agreement with the data over two orders of magnitude in measured heat transfer coefficient.

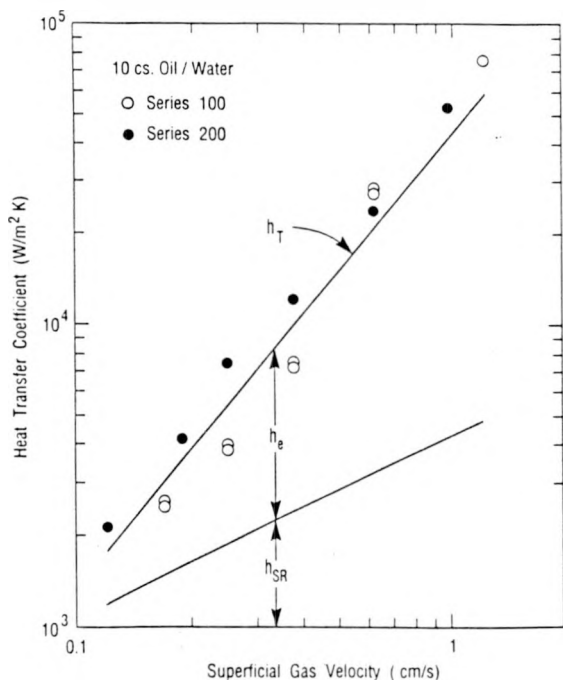


Fig. 6 Measured Overall Heat Transfer vs. Gas Velocity

6. CONCLUSIONS

A framework for evaluating the total heat transfer between overlying immiscible liquid layers with bubble induced entrainment was presented. It was found to be a synthesis of surface renewal heat transfer and that due to direct heat transfer from the entrained drops. Models for surface renewal heat transfer, entrainment onset, and entrainment rate were presented and compared to available experimental data. The models and data were found to be in very good agreement. These models were then combined to construct the overall heat transfer model, Equation 14. When the total interlayer heat transfer model was compared to available heat transfer data for bubbling pools of 10 cs. silicone oil over water, the model and data were found to be in very good agreement over two orders of magnitude in the measured total heat transfer coefficient.

Table 1.

Entrainment Heat Transfer Data
10 cs. Silicone Oil/Water

RUN	J_o (cm/s)	$h_{measured}$ (W/m ² K)
101	0.17	2578
102	0.17	2490
103	0.25	3819
104	0.25	3953
105	0.38	7115
106	0.38	7490
107	0.63	27344
108	0.63	28646
110	1.25	75300
200	0.12	2136
210	0.19	4143
220	0.25	7382
230	0.38	12058
240	0.63	23670
250	1.00	52513

NOMENCLATURE

c_p	specific heat
d_b	spherical equivalent bubble diameter
g	gravity
h	heat transfer coefficient
j_o	superficial entrainment flux
J_o	superficial gas velocity
k	thermal conductivity
K	droplet heat transfer efficiency
Nu	Nusselt number ($=hr_b/k$)
Pr	Prandtl number
r_b	spherical equivalent bubble radius
Re	superficial Reynolds number ($=J_o r_b / \nu$)
Re_o	entrainment Reynolds number
$Re_{1,2}$	bubble Reynolds number in layer 1 or 2 ($=u_b d_b / \nu$)
u_b	bubble rise velocity
V_e	entrained volume
V_b	bubble volume
V_{oo}	entrainment onset bubble volume

V_g^* minimum bubble penetration volume
 $V_{m.}$ maximum theoretical entrainment volume

SUBSCRIPTS

e entrainment
 g gas
 i side of interface, $i = 1$ or 2
 SR surface renewal
 T total
 1 upper light liquid
 2 lower heavy liquid

Greek

ϵ entrainment efficiency
 ρ density
 σ_{12} interfacial tension
 ν kinematic viscosity
 w dimensionless bubble volume
 ϕ dimensionless excess bubble volume

REFERENCES

- Szekely, J. (1963), "Mathematical Model for Heat or Mass Transfer at the Bubble Stirred Interface of Two Immiscible Liquids," *Int. J. Heat Mass Transfer*, 6, pp. 417-422.
- Greene, G.A. and Irvine, T.F. Jr. (1988a), "Heat Transfer Between Stratified Immiscible Liquid Layers Driven by Gas Bubbling Across the Interface," 25th National Heat Transfer Conference, ANS-HTC vol. 3, pp. 31-36.
- Mercier, J.L., da Cunha, F.M., Teixeira, J.C. and Scofield, M.P. (1974), "Influence of Enveloping Water Layer on the Rise of Air Bubbles in Newtonian Fluids," *J. Applied Mechanics*, 96, pp. 29-34.
- Mori, Y.H., Komotori, K., Higeta, K. and Inada, J. (1977), "Rising Behavior of Air Bubbles in Superposed Liquid Layers," *Canadian J. Chem. Engrg.*, 55, pp. 9-12.
- Epstein, M., Petrie, D.J., Linehan, J.H., Lambert, G.A. and Cho, D.M. (1981), "Incipient Stratification and Mixing in Aerated Liquid-Liquid or Liquid-Solid Mixtures," *Chem. Eng. Sci.*, 36, pp. 784-787.
- Suter, A. and Yadigaroglu, G. (1988), "Bubble Driven Mixing of the Oxidic and Metallic Phases During MCCI," *Trans. Am. Nucl. Soc.*, 56, pp. 401-403.
- Greene, G.A., Chen, J.C. and Conlin, M.T. (1988b), "Onset of Entrainment Between Immiscible Liquid Layers Due to Rising Gas Bubbles," *Int. J. Heat Mass Transfer*, 31(6), pp. 1309-1317.
- Poggi, D., Minto, R. and Davenport, W.G. (1969), "Mechanisms of Metal Entrapment in Slag," *J. Metals*, 21, pp. 40-45.
- Cheung, F.G., Leinweber, G. and Pedersen, D.R. (1986), "Bubble-Induced Mixing of Two Horizontal Liquid Layers with Non-Uniform Gas Injection at the Bottom," *Proceedings Sixth Information Exchange Meeting on Debris Coolability*, EPRI NP-4455.
- Veeraburus, M. and Philbrook, W.O. (1959), "Observations on Liquid-Liquid Mass Transfer with Bubble Stirring," in *Physical Chemistry of Process Metallurgy*, Interscience Publishers, New York.
- Greene, G.A., Chen, J.C. and Conlin, M.T. (1990), "Bubble Induced Entrainment Between Stratified Liquid Layers," accepted for publication in *Int. J. Heat Mass Transfer*, 33.
- Greene, G.A. and Schwarz, C.E. (1982), "An Approximate Model for Calculating Overall Heat Transfer Between Overlying Immiscible Liquid Layers with Bubble-Induced Liquid Entrainment," *Proceedings Information Exchange Meeting on Post Accident Debris Cooling*, Karlsruhe, FRG.